1992

Analytical Modeling of Discharge Flow Dynamics in Scroll Compressors

J. J. Nieter
United Technologies Research Center

D. P. Gagne
United Technologies Research Center

ANALYTICAL MODELING OF DISCHARGE FLOW DYNAMICS IN SCROLL COMPRESSORS

Jeff J. Nieter
Research Engineer

Douglas P. Gagne
Assistant Research Engineer

United Technologies Research Center
411 Silver Lane, Mail Stop 129-19
East Hartford, CT 06108

ABSTRACT

The dynamic characteristics of scroll compressor operation have been demonstrated and analyzed in a number of papers over the past decade. This paper discusses the modeling methods used to describe the scroll compressor discharge dynamics. Numerous models are required to accurately represent this complex dynamic process. These include the differential mass continuity and polytropic compression equations for the scroll pockets during compression and discharge, the isentropic flow equation and geometric area open for flow through the discharge port, and acoustic modeling techniques for pressure oscillations in the discharge manifold. The modeling approach is validated by comparison of the predicted compression and discharge pocket pressures with dynamic pressure measurements.

NOMENCLATURE

A	Area
C_D	Discharge coefficient for flow
g_c	Gravitational acceleration
h	Enthalpy of gas
i	Imaginary number
m	Mass of gas
M	Number of discrete manifold sections
$\dot{m}$	Mass flow rate of gas
n_p	Polytropic exponent
N	Number of frequency harmonics
p	Pressure
Q	Volume velocity
$\dot{Q}$	Rate of Heat transfer
SOS	Start of suction process
SOC	Start of 'closed' compression process
SOD	Start of discharge process
EOD	End of discharge process
t	Time
T	Transfer matrix
u	Internal energy of gas
v	Velocity of gas
$\dot{W}$	Rate of boundary work
z	Elevation of gas
Z	Acoustic impedance
θ	Crank angle, or orbit angle position of orbiting scroll
ρ	Density of gas
ω	Angular frequency
ω_o	Fundamental angular frequency
ϕ	Phase angle of mass flow rate and volume velocity harmonics
ψ	Phase angle of pressure pulsation harmonics

Subscripts

c	Control volume, chamber
D	Discharge port
do	Downstream
in,i	Into control volume, manifold
L	Discharge line

out,o Out of control volume, manifold
up Upstream

Superscripts

. First derivative with respect to time
~ Complex quantity
- Average quantity

INTRODUCTION

A common source for noise in many positive displacement type compressors is the oscillatory flow of discharge gas through the discharge porting. This is especially true for hermetic scroll compressors with low side type shells (most of shell interior at suction pressure) due to the relatively small region within the shell for the discharge gas path. Consequently, there is limited space for muffling the discharge flow pulsations. In light of this potential for noise, and in the interest of improving other aspects of compressor performance, it is very important to gain an understanding of the discharge flow dynamics. Analytical modeling is a very good approach to gaining this understanding, as well as producing a tool which can enable the design engineer to improve upon the dynamic behavior of the discharge process.

A number of papers[1] in recent years have discussed various aspects of scroll compressor operation. These discussions have covered the range of topics from thermodynamic effects in terms of leakage, flow losses, compression losses, etc. to structural dynamics in terms of orbiting scroll motion, crankshaft oscillation, and crankcase vibrations. One topic not adequately discussed is the dynamic characteristics and modeling approaches associated with the scroll compressor discharge process and resulting pressure pulsations. In this paper, a detailed description is given of the modeling approach used for the discharge process and the dynamic characteristics associated with this process.

ANALYTICAL MODELING

Geometric Relationships

To model the scroll compression and discharge processes, descriptions of volume in the pair of compression pockets and area open for discharge flow as functions of time are required. These geometric relationships are more conveniently described as functions of scroll orbit angle, or crank angle. Such analytical expressions have been documented to some extent for various wrap geometries in past literature[2-5] and therefore will not be given here. However, a qualitative description of the geometric regions used in our current model, especially for discharge flow area, will be provided for clarification of our approach.

Volume in a pair of scroll pockets is shown in Fig. 1 for a typical scroll compressor from the start of suction (SOS) through the end of discharge (EOD). The process from the start of compression (SOC) to the start of discharge (SOD) is approximately a closed compression process; only leakage, or porting for some pneumatic type operations such as a back chamber[6], prevent it from being truly a closed process. Once the inner wrap tips open at SOD, the control volume in the pockets is no longer 'closed', and the problem of defining a boundary to the control volume in the open regions must be resolved. In Fig. 2 scroll wraps are shown some time after SOD with the cross-sectional area of one pocket control volume shaded. The figure shows the imaginary boundary between the inner wrap tip and mating wrap surface as indicated by the line from P to T. This line is the normal to the inner wrap surface which passes through the mating inner wrap tip at P, and is one of the imaginary boundaries utilized to describe the volume in Fig. 1 after SOD. Additionally, an imaginary boundary is assumed in the plane of the fixed scroll plate which segregates the discharge port from the pocket control volume.

The effective area open for discharge flow in scroll compressors is a complicated problem to describe. Our current approach uses an effective area which is

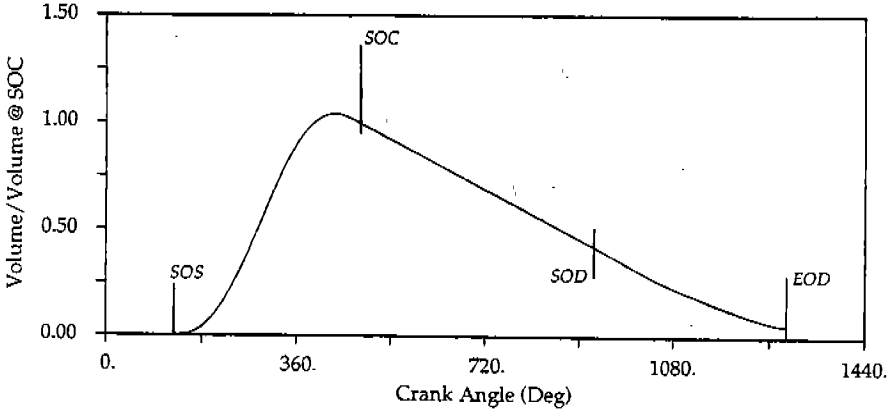

Fig. 1 Volume in a pair of typical scroll pockets from SOS to EOD.

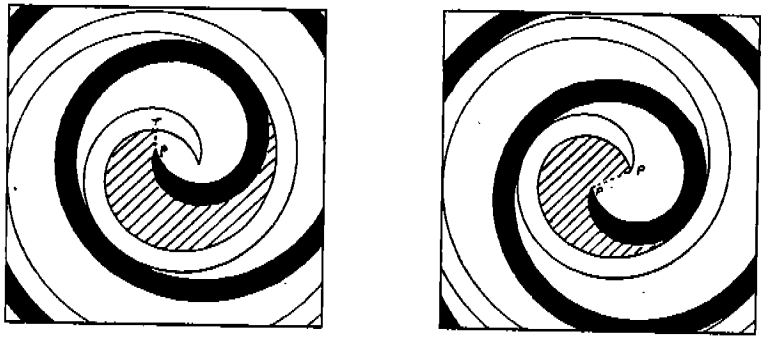

Fig. 2 Control volume in scroll pocket after SOD.

the combination of four different geometric areas that open in various ways during one orbit cycle. These four areas are shown in Figs. 3-6 and are, respectively: (1)the rectangular area formed by the gaps (P to T) between the mating inner wrap tips and the full height of the wrap flanks, (2)the area of the entire discharge port uncovered by the area of the orbiting inner wrap tip, (3)the area of the discharge port outside the orbiting inner tip, and (4)the area of the discharge dimple outside the fixed inner wrap tip. The discharge dimple is a shallow cavity introduced into the orbiting scroll plate in a fashion similar to the port in the fixed scroll plate. The purpose of the dimple is to allow compressed gas to escape under the fixed wrap tip as area (4) is uncovered to provide a more symmetric discharge process. These four types of areas are plotted for one orbit cycle in Fig. 7 for a typical scroll compressor. The first area, A_{D1}, is for just one of the two identical gaps between the inner tips. The third and fourth areas, A_{D3} and A_{D4}, are terminated before completing a full cycle because the definition of these areas is not meaningful for the full cycle. The effective area used for computing discharge flow is plotted in Fig. 8 corresponding to the four area types shown in Fig. 7 and is derived as follows. Initially, the effective area is the sum

$$A_D = 2(A_{D1}) + A_{D3} + A_{D4} \qquad (1)$$

This description is used until A_D equals A_{D2}, after which A_D is simply set to A_{D2}. One further modification is performed: in the transition region around where A_D equals A_{D2}, a procedure is applied to A_D to smooth the curve, resulting in that shown.

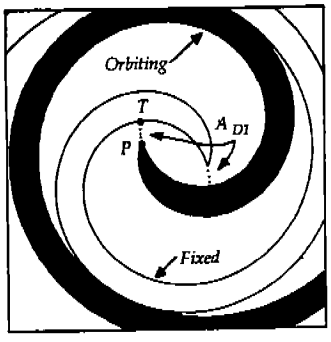

Fig. 3 Discharge flow area type 1

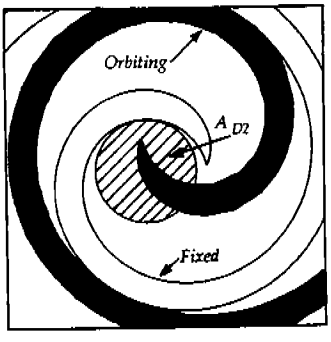

Fig. 4 Discharge flow area type 2

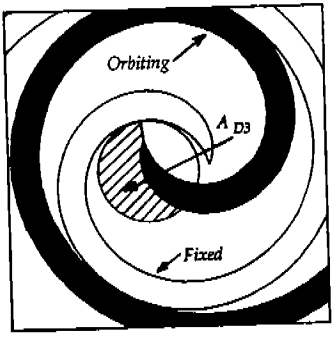

Fig. 5 Discharge flow area type 3

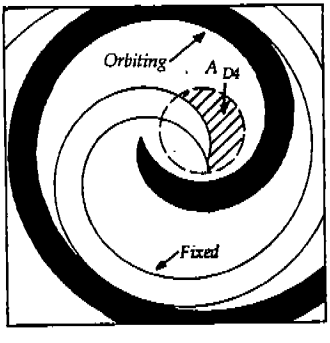

Fig. 6 Discharge flow area type 4

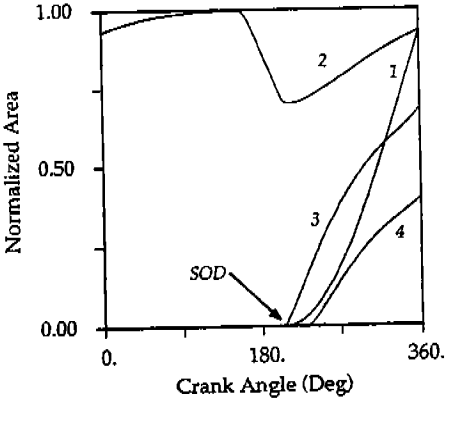

Fig. 7 Variation of individual areas

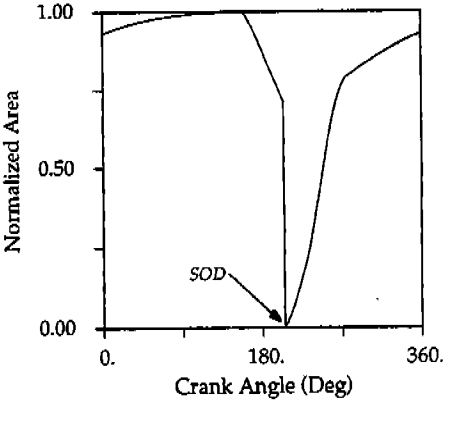

Fig. 8 Effective discharge flow area

Compression Process

The compression process pertains to 'closed' compression after the outer wrap tips seal off at SOC and continues until the inner wrap tips open at SOD. (For a description of the scroll suction process leading up to 'closed' compression, see Reference 7.) Further, compression effectively continues after SOD, through the discharge process until EOD. Therefore, the following relationships that are used to model compression processes are actually applied from SOC to EOD as well. For all process equations, it is assumed that gas properties are uniform throughout each defined region, e.g. properties are uniform throughout the compression and discharge pockets.

The instantaneous mass of gas contained within the control volume for a pair of compression pockets can be described by the differential continuity equation,

$$\frac{dm_c}{dt} = \sum \left(\dot{m}_{in} - \dot{m}_{out} \right) \tag{2}$$

The gas state in the control volume during the compression process normally is modeled by one of two approaches: either using the polytropic process, or using the first law of thermodynamics (energy conservation). The polytropic process model is quite often a good approximation to employ for displacement compressors. It simply uses the relation

$$p_c = p_{SOC} \left(\frac{\rho_c}{\rho_{SOC}} \right)^{n_p} \tag{3}$$

The greatest difficulty with this model is obtaining an accurate value for the polytropic exponent n_p; a good approach is to measure n_p in a laboratory experiment[8].

The first law of thermodynamics on a time rate basis can be applied to the control volume using

$$\frac{d}{dt}\left(m_c u_c\right) = \dot{Q} - \dot{W} + \sum \dot{m}_{in} \left(h + \frac{v^2}{2} + gz \right)_{in} - \sum \dot{m}_{out} \left(h + \frac{v^2}{2} + gz \right)_{out} \tag{4}$$

Application of this approach is more difficult than the polytropic model. The general energy equation given must be reduced to a usable form, typically a differential equation of gas temperature in the control volume. Further, reduction of the general form involves obtaining a number of partial differentials relating enthalpy and pressure to temperature and specific volume[9]. These are trivial for ideal gas properties, but for real gas properties are more difficult to compute. Finally, the greatest obstacle to using Eq. (4) is in obtaining reasonably accurate values of heat transfer $\dot{Q}$. Models used for heat transfer in positive displacement compressors have been fairly well documented for reciprocating piston types[10], but much less so for other types, and apparently not at all for scroll compressors. Currently, the polytropic model is used in our scroll compressor simulation.

Discharge Process

The instantaneous mass flow rate of discharge gas exiting or back-flowing into the control volume can be described using the steady, one-dimensional, isentropic flow equation such as for a nozzle,

$$\dot{m}_D(\theta) = \rho_D A_D C_D \sqrt{2 g_c \left(h_{up} - h_{do} \right)} \tag{5}$$

where A_D is obtained from the procedure described above and C_D is an appropriately chosen flow coefficient[11]. As stated previously, the relationships used to model

the state of the gas in the control volume during the discharge process are the same as those used during the 'closed' compression process.

Discharge Pulsations

Gas pulsations in compressor manifolds have a significant effect upon suction and discharge processes. Modeling this interaction between the discharge flow process and manifold pressure pulsations can be accomplished in a number of ways[12,13]. Probably the most powerful and flexible of these approaches is the transfer matrix method which is performed in the frequency domain[12-16].

In the transfer matrix approach, pressure pulsations are modeled by combining the steady-state acoustical impedance description of the manifold with an acoustical source: the oscillatory gas flow in or out of the port. The power of the transfer matrix approach is that in the frequency domain, analysis consists of complex algebraic operations, rather than solving differential equations with associated boundary conditions in the time domain. Since the mass flow rate through the discharge port is a periodic function of time or crank angle, it can be represented by a finite Fourier series[14,15]

$$\dot{\tilde{m}}_D(\theta) = \dot{m}_D(0) + \sum_{n=1}^{N} |\dot{\tilde{m}}_D(n\omega_o)| \exp i\left(n\theta + \phi_D(n\omega_o) \right) \tag{6}$$

The actual acoustic source used in the analysis is volume velocity $\tilde{Q}_D$ which is represented similarly as

$$\tilde{Q}_D(\theta) = Q_D(0) + \sum_{n=1}^{N} |\tilde{Q}_D(n\omega_o)| \exp i\left(n\theta + \phi_D(n\omega_o) \right) \tag{7}$$

where

$$|\tilde{Q}_D(\omega)| = |\dot{\tilde{m}}_D(\omega)| \; / \; \bar{\rho}_D \tag{8}$$

The transfer matrix approach uses the four-pole or two-port network theory to cascade, by transfer matrices, the acoustic elements of the discretized manifold. An example of a discretized manifold is depicted in Fig. 9 where the corresponding cascade of transfer matrices would be

$$\begin{Bmatrix} \tilde{p}_i(\omega) \\ \tilde{Q}_i(\omega) \end{Bmatrix} = \tilde{T}_1 \, \tilde{R}_2 \, \tilde{T}_3 \, \tilde{R}_4 \, \tilde{T}_5 \, \tilde{T}_6 \begin{Bmatrix} \tilde{p}_o(\omega) \\ \tilde{Q}_o(\omega) \end{Bmatrix} = \tilde{T}_M \begin{Bmatrix} \tilde{p}_o(\omega) \\ \tilde{Q}_o(\omega) \end{Bmatrix} \tag{9}$$

where

$$\tilde{T}_k = \begin{bmatrix} \tilde{A}_k(\omega) & \tilde{B}_k(\omega) \\ \tilde{C}_k(\omega) & \tilde{D}_k(\omega) \end{bmatrix}, \text{ for each } k = 1, 2, \ldots, 6, M \tag{10}$$

and

$$\tilde{R}_k = \begin{bmatrix} 1 & 0 \\ \tilde{C}_k/\tilde{A}_k & 1 \end{bmatrix}, \text{ for } k = 2, 4. \tag{11}$$

Here, $\tilde{R}_k$ is the transfer matrix of the side branches for the extended-tube resonators 2 and 4. Each transfer matrix $\tilde{T}_k$ describes the acoustic properties of the discrete manifold section it represents, within the limitations of the acoustic theory employed for that section. This is another major factor adding to the power of this approach: since manifolds are discretized into acoustic elements, only the sophistication of the types of elements available limit the complexity of the

manifolds which can be accurately modeled. Commonly used acoustic elements[16] consist of one-dimensional distributed parameter types (e.g., a constant cross-sectional area duct) as well as lumped parameter types (e.g., a resonator volume).

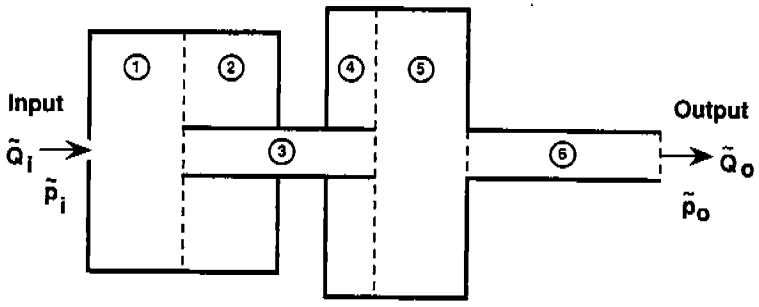

Fig. 9 Example discretized manifold system

In recent years, three-dimensional effects have been utilized[17,18] to describe the acoustical impedances of manifolds when accounting for cross modes in larger sized regions for higher frequency prediction capability. The most flexible implementation of 3-D effects would be to use the transfer matrix method to analyze the whole manifold system, but use some other analysis procedure capable of 3-D acoustic analysis to obtain the four-pole parameters of the large sized sections. These four-pole parameters containing the 3-D effects of large sections can be input into the transfer matrix analysis for the whole manifold system.

From the transfer matrix of the whole manifold system $\bar{T}_M$, the steady-state acoustic impedances for the manifold can be obtained[14,15]. The driving point impedance at the input location is,

$$\bar{Z}_{ii}(\omega) = \frac{\bar{p}_i(\omega)}{\bar{Q}_i(\omega)} = \frac{\bar{p}_D(\omega)}{\bar{Q}_D(\omega)} = \frac{\bar{A}_M(\omega)}{\bar{C}_M(\omega)} \tag{12a}$$

and the cross point impedance to the output location is,

$$\bar{Z}_{oi}(\omega) = \frac{\bar{p}_o(\omega)}{\bar{Q}_i(\omega)} = \frac{\bar{p}_L(\omega)}{\bar{Q}_D(\omega)} = \frac{1}{\bar{C}_M(\omega)} \tag{12b}$$

By combining the acoustic impedances with the source (oscillatory gas flow), the oscillatory part of the gas pressures can be obtained[14,15],

$$\tilde{p}_D(\omega) = \bar{Z}_{ii}(\omega)\ \tilde{Q}_D(\omega) \tag{13a}$$

$$\tilde{p}_L(\omega) = \bar{Z}_{oi}(\omega)\ \tilde{Q}_D(\omega) \tag{13b}$$

These pressure harmonics $p(\omega)$ can then be represented back in the time (or crank angle) domain using the Fourier series[14,15],

$$p_D(\theta) = \bar{p}_D + \sum_{n=1}^{N} |\bar{p}_D(n\omega_o)| \cos\left(n\theta + \psi_D(n\omega_o) \right) \qquad (14)$$

Consequently, pressure pulsations in the discharge manifold are modeled and coupled to the oscillating gas flow through the discharge port. This concludes the summary of the primary models used in our comprehensive scroll compressor simulation which are pertinent to discharge flow dynamics.

SCROLL DISCHARGE CHARACTERISTICS

The dynamic character of discharge gas flow and the resulting pressure pulsations in standard scroll compressors without discharge valves are notably different from that occurring in compressors with discharge valves. This is because standard scroll compressors are fixed volume ratio machines. Consequently, discharge flow characteristics are dependent entirely upon the mismatch between the compressor and system pressure ratios, and the flow area available for equalization of this pressure mismatch. The flow area available is dictated by the geometry of the port and inner scroll wraps as described above.

The oscillatory flow which emanates from the discharge port acts as a forcing function to the dynamic system consisting of the acoustic transmission path in the discharge gas and the structural path of the compressor shell assembly. Consequently, this oscillatory discharge flow can be a prominent noise source in scroll compressors. Contained in this oscillatory flow, for some operating conditions, is a large flow pulse at the start of the periodic discharge process. The largest pulses in gas flow occur at system pressure ratios much higher than that of the compressor due to the sudden back flow which takes place for pressure equalization. An example of the severity of such a back-flow pulse, as predicted by our simulation, is shown in Fig. 10 by the solid curve. These back-flow pulses are also of short time duration and therefore, contain energy at high frequencies, as is clear in the frequency spectrum of Fig. 11 corresponding to the solid curve of Fig. 10. At system pressure ratios which are significantly less than the compressor's, a broad over-pressure pulse is generated as shown by the dashed curve in Fig. 10. The frequency spectrum for this mass flow rate time history is given in Fig. 12 and shows the significantly lower harmonic content characteristic of over-pressure pulses.

It is a matter of course that the pressure pulsations resulting from oscillatory gas flow containing back-flow pulses as in Fig. 11 are more likely to generate noise problems than may occur from oscillatory flow containing over-pressure pulses as in Fig. 12. From a gas pulsation viewpoint, one would be inclined to minimize the abrupt back flow due to pressure equalization by maximizing the machine's pressure ratio for the range of system pressure ratios expected. This would increase the range of conditions where over-pressure pulses and lower gas pulsation harmonics occur (a positive noise reduction effect), but also would increase the over-pressure losses at these conditions (a negative efficiency effect).

In Figs. 13 and 14, the pressure-volume diagrams corresponding to the conditions and mass flow histories of Fig. 10 are shown. The dramatic increase in scroll pocket pressure shortly after SOD due to the strong back flow is apparent in Fig. 13. This back-flow effect results in a large increase in compression power over what would be required if the compressor pressure ratio matched the system. The area between the solid curve and the dashed curve in Fig. 13 represents this increase in compression power. The total compression power is proportional to the enclosed pressure-volume area. In Fig. 14, the pocket pressure after SOD increases more gradually due to normal flow and over-pressure before peaking and then slowly decreasing back to discharge pressure. There is no increase in power due to back flow, only the increase in compression power due to over-pressure. The area between the pocket pressure curve and the discharge pressure curve in both figures represents the increase in compression power due to over-pressure. The power due to over-pressure in Fig. 14 is clearly greater than that in Fig. 13.

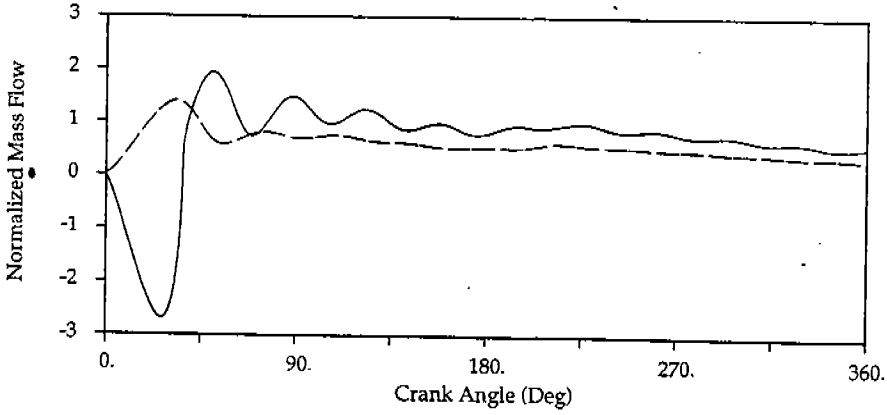

Fig. 10 Discharge mass flow rate during one orbit cycle for condition where system pressure ratio is much greater than the compressor (solid curve) and for one where system pressure ratio is less than the compressor (dashed curve)

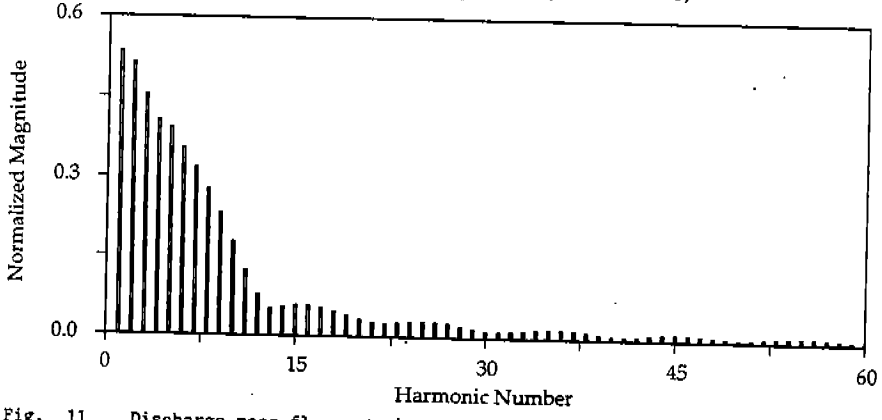

Fig. 11 Discharge mass flow rate harmonic magnitudes for condition where system pressure ratio is much greater than the compressor

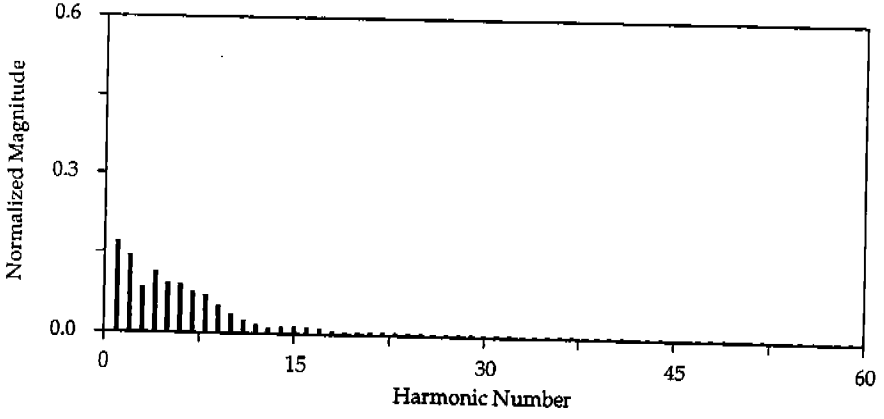

Fig. 12 Discharge mass flow rate harmonic magnitudes for condition where system pressure ratio is less than the compressor

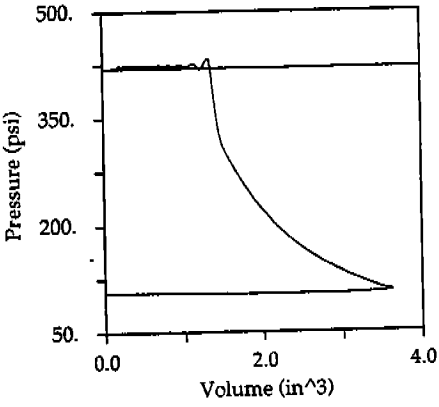

Fig. 13 Pressure-volume diagram for condition where system pressure ratio is much greater than the compressor

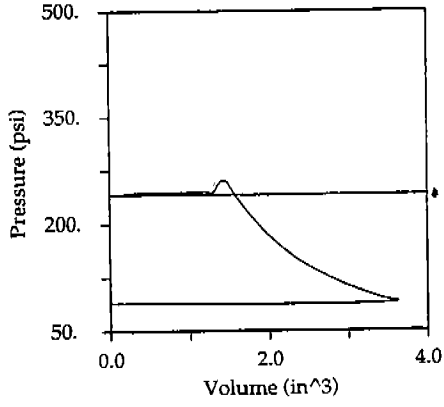

Fig. 14 Pressure-volume diagram for condition where system pressure ratio is less than the compressor

Thus we see the dilemma: though discharge flow pulses, which cause pressure pulsations, are less likely to be a problem for a compressor with a pressure ratio greater than (or equal to) that of the system. When considering the full range of operating conditions, the power required for compression may be much greater than for a lower pressure ratio machine. Consequently, the design engineer has to compromise between discharge gas pulses and compressor efficiency. If considerable flow pulses still exist after completing a design, the next step is to address the transmission paths whereby this gas pulsation energy is transmitted to the outside world. Proper design of the discharge manifold from an internal acoustics viewpoint (manifold tuning[15]) can address the gas transmission path. Finally, the vibratory characteristics of the compressor shell can be modified to reduce the transmission of gas pulsation energy through this path.

MODEL VALIDATION

The models described here are part of a comprehensive scroll compressor simulation. Predictions from this simulation have been validated by comparison with data measured in the laboratory[8,19]. Typical comparisons between measured and predicted pocket pressures from SOS to EOD are shown in Fig. 15 for the ARI condition and in Fig. 16 for the 45/110 condition. (Predicted pressures are represented with dashed curves and measured pressures are represented with solid curves.) As can be observed in these figures, there is excellent agreement between predicted and measured pressure dynamics. Also, it should be noted that the pressure pulsations shown in Figs. 15 and 16 are of much greater amplitude than occur in a production hermetic compressor because of the shell configuration required in the laboratory for transducer feed-throughs. No measurements of discharge mass flow dynamics are currently available for comparison with that predicted, nor have they been documented for scroll compressors in the literature - this is an area for future work.

CONCLUSIONS

The scroll compression and discharge process modeling approaches were discussed along with approaches for modeling discharge pressure pulsations. The discharge gas flow pulsations can be a significant noise source in scroll compressors. Proper understanding of the dynamic character during scroll discharge can be very beneficial in avoiding possible noise problems. These discharge flow dynamics are due primarily to the mismatch between the system and compressor pressure ratios, and the flow area available for equalization of this mismatch. The models presented here provide greater insight and act as a tool for controlling this phenomena. Further, the modeling approach has been validated with measured pressure data.

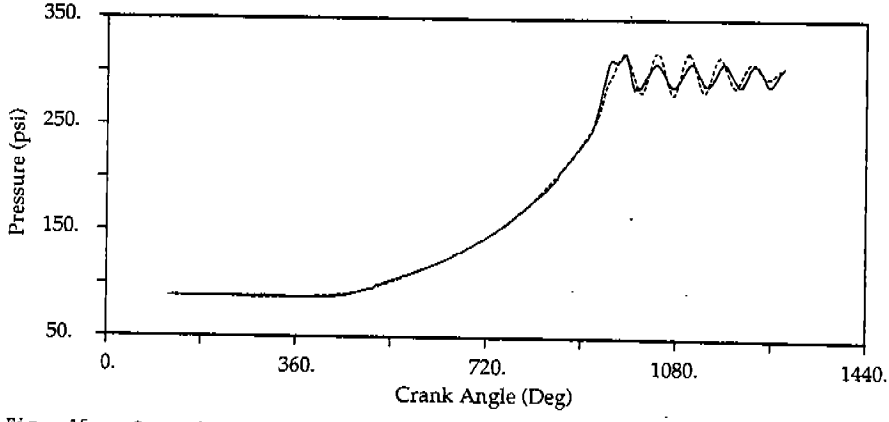

Fig. 15 Comparison of predicted and measured scroll pocket pressure from SOS to EOD at ARI condition (solid curve is measured, dashed curve is predicted)

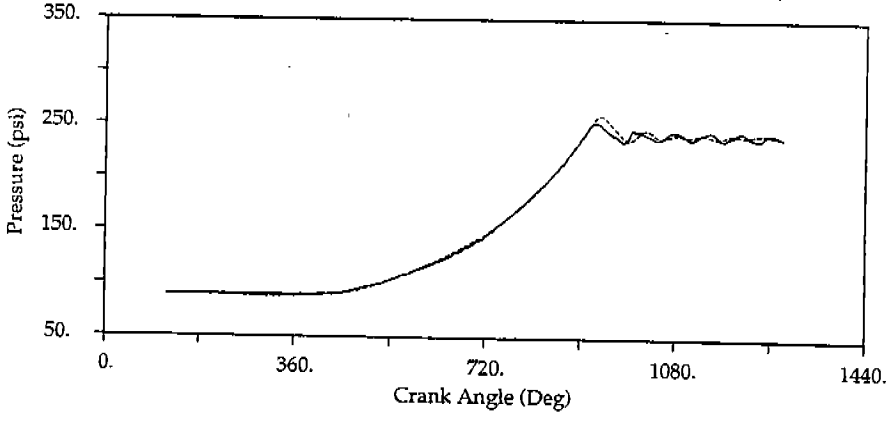

Fig. 16 Comparison of predicted and measured scroll pocket pressure from SOS to EOD at 45/110 condition (solid curve is measured, dashed curve is predicted)

REFERENCES

1. Proceedings of the International Compressor Engineering Conference at Purdue, 1984 - 1990.
2. Morishita, E., et al., "SCROLL COMPRESSOR ANALYTICAL MODEL", Proc. of the 1984 Intern. Compr. Eng. Conf. (Purdue), July 1984, pp. 487-495.
3. Hayano, M., et al., "PERFORMANCE ANALYSIS OF SCROLL COMPRESSOR FOR AIR CONDITIONERS", Proc. of the 1986 Intern. Compr. Eng. Conf. (Purdue), Aug. 1986, pp. 856-871.
4. Tojo, K., et al., "COMPUTER MODELING OF SCROLL COMPRESSOR WITH SELF ADJUSTING BACK-PRESSURE MECHANISM", Proc. of the 1986 Intern. Compr. Eng. Conf. (Purdue), Aug. 1986, pp. 872-886.
5. Yanagisawa, T., et al., "OPTIMUM OPERATING PRESSURE RATIO FOR SCROLL COMPRESSOR", Proc. of the 1990 Intern. Compr. Eng. Conf. (Purdue), July 1990, pp. 425-433.
6. Nieter, J.J. and Barito, T., "DYNAMICS OF COMPLIANCE MECHANISMS IN SCROLL COMPRESSORS PART I: AXIAL COMPLIANCE", Proc. of the 1990 Intern. Compr. Eng. Conf. (Purdue), July 1990, pp. 308-316.
7. Nieter, J.J., "DYNAMICS OF SCROLL SUCTION PROCESS", Proc. of the 1988 Intern. Compr. Eng. Conf. (Purdue), July 1988, pp. 165-174.
8. DeBlois, R.L. and Stoeffler, R.C., "INSTRUMENTATION AND DATA ANALYSIS TECHNIQUES FOR SCROLL COMPRESSORS", Proc. of the 1988 Intern. Compr. Eng. Conf. (Purdue), July 1988, pp. 182-188.

9. Ng, E.H., et al., "COMPUTER SIMULATION OF A RECIPROCATING COMPRESSOR USING A REAL GAS EQUATION OF STATE", Proc. of the 1980 Purdue Compr. Tech. Conf., July 1980, pp. 33-42.
10. Keribar, R. and Morel, T., "HEAT TRANSFER AND COMPONENT TEMPERATURE PREDICTION IN RECIPROCATING COMPRESSORS", Proc. of the 1988 Intern. Compr. Eng. Conf. (Purdue), July 1988, pp. 454-463.
11. Rodgers, R.J. and Wagner, T.C., "SCROLL COMPRESSOR FLOW MODELING: EXPERIMENTAL AND COMPUTATIONAL INVESTIGATION", Proc. of the 1990 Intern. Compr. Eng. Conf. (Purdue), July 1990, pp. 206-215.
12. Singh, R. and Soedel, W., "A REVIEW OF COMPRESSOR LINES PULSATION ANALYSIS AND MUFFLER DESIGN RESEARCH, PART II - ANALYSIS OF PULSATING FLOWS", Proc. of the 1974 Purdue Compr. Tech. Conf., July 1974, pp. 112-123.
13. Soedel, W., "GAS PULSATIONS IN COMPRESSOR AND ENGINE MANIFOLDS", Short Course Text Book of Purdue Compr. Tech. Conf., Ray W. Herrick Laboratories, Purdue University, 1978.
14. Singh, R. and Soedel, W., "MATHEMATICAL MODELING OF MULTICYLINDER COMPRESSOR DISCHARGE SYSTEM INTERACTIONS", Journal of Sound and Vibration, 1979, 63(1), 125-143.
15. Nieter, J.J. and Singh, R., "A COMPUTER SIMULATION STUDY OF COMPRESSOR TUNING PHENOMENA", Journal of Sound and Vibration, 1984, 97(3), 475-488.
16. Munjal, M.L., ACOUSTICS OF DUCTS AND MUFFLERS WITH APPLICATION TO EXHAUST AND VENTILATION SYSTEM DESIGN, John Wiley & Sons, 1987.
17. Kim, J. and Soedel, W., "FOUR POLE PARAMETERS OF SHELL CAVITY AND APPLICATION TO GAS PULSATION MODELING", Proc. of the 1988 Intern. Compr. Eng. Conf. (Purdue), July 1988, pp. 331-337.
18. Koai, K. and Soedel, W., "GAS PULSATIONS IN TWIN SCREW COMPRESSORS - PART II: DYNAMICS OF DISCHARGE SYSTEM AND ITS INTERACTION WITH PORT FLOW", Proc. of the 1990 Intern. Compr. Eng. Conf. (Purdue), July 1990, pp. 378-387.
19. Hirano, T., et al., "DEVELOPMENT OF HIGH EFFICIENCY SCROLL COMPRESSORS FOR AIR CONDITIONERS", Proc. of the 1988 Intern. Compr. Eng. Conf. (Purdue), July 1988, pp. 65-74.